Dynamical Scenarios for Chromosome Bi-orientation

Tongli Zhang, Raquel A. Oliveira[1], Bernhard Schmierer[2] and Béla Novák

Oxford Centre for Integrative Systems Biology, Department of Biochemistry, University of Oxford, Oxford, United Kingdom

[1]Raquel A. Oliveira's current address is Instituto Gulbenkian de Ciência, Rua da Quinta Grande, 6; P-2780-156 Oeiras, Portugal.

[2]Bernhard Schmierer's current address is Department of Biosciences and Nutrition, Karolinska Institutet, SE-141 83 Stockholm, Sweden.

Abstract

Chromosome bi-orientation at the metaphase spindle is essential for precise segregation of the genetic material. The process is error-prone, and error-correction mechanisms exist to switch misaligned chromosomes to the correct, bi-oriented configuration. Here, we analyze several possible dynamical scenarios to explore how cells might achieve correct bi-orientation in an efficient and robust manner. We first illustrate that tension-mediated feedback between the sister kinetochores can give rise to a bistable switch, which allows robust distinction between a loose attachment with low tension and a strong attachment with high tension. However, this mechanism has difficulties in explaining how bi-orientation is initiated starting from unattached kinetochores. We propose four possible mechanisms to overcome this problem (exploiting molecular noise; allowing an efficient attachment of kinetochores already in the absence of tension; a trial-and-error oscillation; and a stochastic bistable switch), and assess their impact on the bi-orientation process. Based on our results and supported by experimental data, we put forward a trial-and-error oscillation and a stochastic bistable switch as two elegant mechanisms with the potential to promote bi-orientation both efficiently and robustly.

Introduction

During each cell cycle, the cellular genome is first replicated and then spatially segregated into the two daughter cells. The formation of the microtubule-based spindle machinery and the capture of chromosomes are complex processes that have been studied experimentally and theoretically (1, 2, 3, 4, 5). To ensure that each daughter cell receives one and only one copy of the replicated genome, each duplicated chromosome must bi-orient at the mitotic spindle, with its sister chromatids attached to microtubules originating from opposite spindle poles (2). This so-called amphitelic attachment guarantees that sister chromatids are pulled into opposite directions once the cohesion between them is severed at the meta- to anaphase transition (6, 7).

Geometric properties are likely to bias sister chromatids toward an amphitelic attachment configuration (8, 9, 10, 11). Nevertheless, it is possible for microtubules originating from one spindle pole to bind to both sister kinetochores, a situation that is referred to as syntelic attachment. Similarly, a single kinetochore can be bound simultaneously by microtubules from both spindle poles, which is referred to as merotelic attachment. If uncorrected, such faulty attachment configurations will result in aneuploid daughter cells and genetic instability (12, 13). To avoid this deleterious scenario, cells have evolved error correction mechanisms to recognize and rectify erroneous attachment configurations.

At the molecular level, Aurora B, the kinase component of the chromosomal passenger complex, is a critical mediator of the release of erroneous kinetochore-microtubule (KT-MT) attachments (14, 15). If

Aurora B activity is reduced, incorrect attachments accumulate (16, 17, 18, 19). The selective dissolution of erroneous, but not amphitelic attachment configurations implies that Aurora B, and/or other proteins involved in the process, can distinguish between these two cases.

Tension between sister kinetochores is one feature that distinguishes amphitelic from syntelic attachments and, at least in its degree or directionality, also from merotelic attachment configurations (20). This tension is created by the KT-MT attachments and a pulling force toward opposite spindle poles, and the resistance exerted by sister chromatid cohesion (21, 22, 23). There is good evidence that KT-MT attachments that are under sufficient tension are less susceptible to dissolution. Possible mechanisms include the direct repression of Aurora B activity at attachment sites that are under tension, and/or tension-dependent spatial separation of centromeric Aurora B from its relevant substrate(s) (24, 25, 26). The tension hypothesis thus states that an amphitelic attachment configuration is stabilized because of the tension it experiences, which is also consistent with the fact that when a microneedle is used to generate tension artificially, then normally unstable, syntelic attachments are stabilized (3, 27). Despite its wide acceptance, the tension hypothesis is a simplification that is unable to successfully explain the resolution of merotelic attachments despite such attachments being under a certain amount of tension (13, 28, 29, 30). Nevertheless, the tension hypothesis is consistent with a large amount of data, even though not all details are understood. Ideally, a control system of bi-orientation should give rise to the following features: Firstly, correct attachment configurations must be clearly distinguishable from incorrect configurations; Secondly, biorientation should be initiated effectively. Thirdly, once established, the bi-oriented state should be stably maintained.

To understand dynamically how the tension hypothesis could give rise to these features, we translated it into a mathematical model. We illustrate that tension-dependent inhibition of a detaching activity, as proposed in the tension hypothesis, creates a positive feedback loop between sister kinetochores, in which attachment on one side stabilizes attachment on the sister side. This feedback system can act as a bistable switch with two steady states: one corresponding to a loose attachment with low tension, and the other to a strong attachment with high tension. This allows a robust distinction between these two states. However, we find that this mechanism does not successfully explain how bi-orientation is initiated from unattached kinetochores. We propose several alternative routes as to how cells might overcome this problem, and compare these scenarios with regard to the required efficiency and robustness of the bi-orientation process. Backed by experimental data, our results point to a trial-and-error oscillation or a stochastic bistable switch as two possible mechanisms that can both efficiently initiate and robustly maintain bi-orientation. Our theoretical work makes testable predictions, and we suggest experiments to support or refute our working model. In combination with the dynamical analysis presented here, the results of suggested experiments will provide valuable insights into the mechanism of the bi-orientation process.

Results

In simplified form, the chromosome alignment process in metaphase according to the tension hypothesis can be described by the interaction of three dynamical entities or variables: Tension, the force experienced by a kinetochore which is proportional to the degree of attachment and the activity of motor proteins, and an activity that detaches attachments that are under insufficient tension.

We call these three dynamical variables Tension, Att and Eraser, respectively. Tension arises from attachments on both kinetochores, the pulling force of motor proteins, and the resisting cohesin at bi-

oriented chromosomes. The variable Att exists only at kinetochores that are attached to microtubules, and it increases with growing numbers of KT-MT attachments as well as with the activity of motor proteins. Eraser is an activity that is localized to a specific kinetochore, and which reduces Att at this specific kinetochore. At the molecular level, there is good evidence that Aurora B is an important component of the Eraser activity (16, 17,18, 19), which, however, is not sufficient (35). Aurora B substrates that have been implicated in the regulation of the stability of KT-MT attachments are, among others, the kinetochore protein Ndc80/Hec1 (36, 37) and the kinesin-13 family member MCAK (38, 39). In our simplified model, we use the general term "Eraser" without elaborating on its molecular composition and exact molecular function.

Two double-negative feedback loops characterize the bi-orientation control network

In the network diagram describing one duplicated chromosome, i.e., two sister chromatids (Fig. 1 *A*), we consider five dynamical variables: Att and Eraser for one kinetochore, S-Att and S-Eraser for the sister kinetochore, and the shared variable Tension. At each of the kinetochores Eraser inhibits Att. Att together with S-Att creates Tension, and Tension inhibits both Eraser and S-Eraser. The system is characterized by two double-negative feedback loops:

$$att \rightarrow ten \dashv era \dashv att;$$
$$S\text{-}att \rightarrow ten \dashv S\text{-}era \dashv S\text{-}att.$$

Moreover, these double-negative feedback loops share the variable Tension and are thus mutually dependent on each other.

The mutual antagonism between Att and Eraser requires *S-Att*

We focus first on the tension-dependent mutual antagonism between Att and Eraser on one of the sister kinetochores. To do this, we treat S-Att and S-Eraser as parameters, assume that Tension is at steady state, and plot the balance curves for Att (*blue line*) and for Eraser (*red line*) on a phase plane (Fig. 1 *B*). Along the balance curves, the respective variable does not change its value. Because Eraser inhibits Att, an increase in Eraser causes a decrease in Att. The shape and position of this curve remains unchanged, whether or not there is attachment at the sister kinetochore. The shape of the Eraser balance curve by contrast is affected by the state of the sister kinetochore. In the absence of sister attachment, an increase in Att does not create any Tension and Eraser remains constantly high, independently of the value of Att. In the presence of S-Att, however, an increase in Att generates Tension. Now Eraser decreases with increasing Att. The intersection of the balance curves marks the steady state of the system. In the absence of S-Att, the steady state is characterized by high Eraser activity and low Att (*open circle*), corresponding to a loose KT-MT binding. In the presence of high S-Att by contrast, the steady state is found at low Eraser activity and high Att, corresponding to a strong KT-MT binding (*solid circle*). In summary: in the absence of a pulling force at the sister kinetochore, there is

no Tension, Eraser is constantly high, inhibiting Att; and the formed attachment is weak. In the presence of attachment at the sister kinetochore, Tension is created and Att inhibits Eraser, giving rise to strong attachment.

To illustrate the effect of an increasing pulling force at the sister kinetochore (increasing S-Att) on Att, we plot Att as a function of S-Att (Fig. 1 *C*). Because this signal-response curve is sigmoid, Att and S-Att are either both low or both high, corresponding respectively to a weak KT-MT attachment if the pulling force from the sister kinetochore is missing or insufficient, and a strong, stabilized KT-MT attachment when the sister kinetochore is being actively pulled. The two states are separated by a threshold, above which the KT-MT attachment is stabilized. The steepness of this threshold depends on the regulatory strengths of the reactions; however, its existence is supported by micromanipulation experiments, where unstable KT-MT attachments become stabilized only by strong forces applied by a needle (3). Here, we assume a steep threshold, because this gives a good differential between the two states, which is arguably an important property of the system. The case of a flat threshold is explored in detail below.

The mutual activation of Att and S-Att can give rise to a bistable switch

Up to now, we have focused on one single kinetochore. However, the two feedback loops operating at the two sister kinetochores are coupled to each other. S-Att promotes the formation of Att, and vice versa. To analyze the effect of this mutual activation in the complete system, i.e., on two sister kinetochores coupled by tension, we reduce the system to two ordinary differential equations, one for Att and one for S-Att. We do this by computing Tension, Eraser, and S-Eraser at their steady states, and plot the Att and the S-Att balance curves on a phase plane (Fig. 1 *D*). The Att balance curve is identical to the signal response curve (Fig. 1*C*), while the S-Att balance curve is a mirror image due to the symmetric regulation. As before, steady states of the system are found at the intersection of the two balance curves. In the case presented, we find two stable steady states separated by an unstable one, indicating that the system is bistable.

The bottom-left steady state (Fig. 1 *D*, *open circle*) indicates a state where both Att and S-Att are low. Because the S-Att level is low, newly formed Att cannot generate sufficient tension to repress Eraser, and Eraser remains active. The same applies symmetrically for S-Eraser. High Eraser and S-Eraser activities destabilize newly formed Att and S-Att, and the state of low Att and low S-Att is self-sustaining. The upper-right steady state (Fig. 1 *D*, *solid circle*) corresponds to the bi-oriented steady state where both Att and S-Att are high. Now Att and S-Att cooperate to repress both Eraser and S-Eraser. Hence,

the state with both high Att and high S-Att is also self-sustaining. These two self-sustaining states are mutually exclusive, and the system will approach either one or the other, depending on its initial state. The two attraction basins of the steady states are separated by a separatrix that extends from an unstable saddle point (Fig. 1 *D*,*open square*). As long as the system initiates within the right attraction basin, the mutual activation of Att and S-Att will stabilize each other and the system will reach stable bi-orientation, with both Eraser and S-Eraser inhibited. On the other hand, if the system initiates within the left attraction basin, it will be attracted to the steady state corresponding to low Att and low S-Att. In this state, both Eraser and S-Eraser are high, and the KT-MT attachments are unstable.

In summary, the system is, in principle, capable of exhibiting bistability, which would guarantee robust switching between two incompatible states - a set of kinetochores under no or low tension that are only loosely attached, and a set of kinetochores that are under high tension and thus strongly attached. While the capability of robust distinction is an important property, the dynamical picture also illustrates a weakness of this switch model. The initial state in chromosome bi-orientation is one in which both Att and S-Att are either weak or absent. Thus, the starting point is necessarily within the attraction basin of the lower steady state, and the system can never reach the upper steady state. Under such circumstances, bi-orientation cannot be initiated; we refer to this as the “initiation problem”. In the following two sections, we propose two alternative sets of modifications to the system that can solve this problem: first, stochastic processes might allow overcoming the separatrix; and second, the positive feedback between Att and S-Att could be weaker, thus precluding bistability altogether.

A stochastic system can cross the separatrix and initiate bi-orientation

As explained above, the separatrix separates two distinct states and cannot be crossed in a deterministic system. However, because binding and unbinding of microtubules to kinetochores are stochastic processes involving low numbers of molecules, attachments on both sides could, by chance, become strong enough to cause bi-orientation. To investigate the stochastic processes of binding and unbinding of microtubules to kinetochores, we have transformed the deterministic model into a stochastic version (for details, see Methods). We start the stochastic simulations from low Att values and high Eraser activities to mimic biologically relevant initial conditions without KT-MT attachments. A representative stochastic simulation shows that, under these conditions, Tension is repeatedly created and lost (Fig. 2 *A*).

To better understand the stochastic dynamics, we plot the system's trajectory for the representative stochastic simulation on the phase plane shown in Fig. 1 *D*. The system starts within the left attraction basin, and is attracted by the stable steady state with low Att and low S-Att (Fig. 2 *B*). Eventually, a coincidental simultaneous increase of Att and S-Att pushes the system across the separatrix and into the attraction basin of the steady state corresponding to bi-orientation. The phase-plane plotting illustrates a potential risk associated with such stochasticity: if stochastic effects are strong enough to cause the system to cross the separatrix, they can also cause the system to cross back, leading to loss of Tension, activation of the Erasers, and loss of bi-orientation. In summary, the stochasticity of the reactions can likely overcome the initiation problem and allow bi-orientation; however, bi-orientation achieved under such circumstances is unstable and can be potentially lost.

Bi-orientation becomes the only steady state if KT-MT attachment is highly efficient

As explained above, a bistable system would allow cells to clearly distinguish correct from incorrect attachment configurations. Importantly, however, whether the system is bistable depends on the regulatory strengths in the network: bistability is a possible but not necessary consequence of the network structure. If, for instance, substantial Att can already be created in the absence of tension (a scenario that is simulated by increasing the parameter R_0^{att}), the signal-response curve loses its sharp threshold (Fig. 2 *C*) and bistability is lost (Fig. 2 *D*). The system has now only a single stable steady state at the upper right, which corresponds to the bi-oriented steady state where both Att and S-Att are high and cooperate in repressing both Eraser and S-Eraser. This state is a self-sustaining, global attractor, and corresponds to the bi-oriented state. Under such circumstances, bi-orientation will eventually form, independently of where the system initiates. However, the relatively strong attachments that are formed already in the absence of Tension (Fig. 2 *C*) are hard to resolve, so a clear distinction of correct and incorrect configurations becomes more difficult.

In summary, the presence of molecular noise in the context of a bistable system, or a mono-stable system are two feasible ways to achieve bi-orientation of a duplicated chromosome. However, both mechanisms have their drawbacks: the noisy bistable system allows spontaneous loss of bi-orientation, and the mono-stable system is inferior in distinguishing between correct and incorrect configurations. These shortcomings prompted us to look for additional design principles that could achieve both faithful and efficient chromosome bi-orientation.

Isolated chromatids experience oscillatory or fluctuating forces

Recent experimental data have revealed apparently oscillatory movements of single chromatids when cells undergo what is referred to as pseudo-anaphase (34). In these experiments, cells expressing a modified cohesin that is cleavable by Tobacco Etch Virus protease are arrested in metaphase by repressing the APC:CDC20 degradation machinery. Arrested cells are then injected with Tobacco Etch Virus protease, which causes cleavage of the modified cohesins and separation of sister chromatids (i.e., pseudo-anaphase, in the sense that sister chromatid cohesion is lost, but cyclin B is not degraded as in normal anaphase). Loss of tension in the presence of cyclin B-dependent mitotic phosphorylations also reactivates the mitotic checkpoint (40).

Interestingly, in these experiments, the centromeric localization of Aurora B closely correlates with the oscillatory movements of isolated chromatids (34), suggesting changes in the spindle pulling force, perhaps as a consequence of periodic changes in attachment strength. We analyzed the data by recording the positions of moving chromatids relative to a reference point (Fig. 3 *A*) and calculated their changing velocities over time (Fig. 3 *B*). Indeed, we find oscillating velocities of isolated chromatids (Fig. 3 *B*). Because in the viscous cellular environment, chromatid velocity is linearly proportional to the force experienced (41), these periodic changes are likely to reflect oscillatory spindle-pulling forces acting on isolated chromatids. These observations suggest that the KT-MT attachment of an isolated kinetochore during pseudo-anaphase might be subject to oscillatory cycles of attachment and detachment. Similar oscillatory movements have been observed also during anaphase in *Drosophila* embryos expressing nondegradable cyclin B (42).

Two appealing dynamical explanations for the observed oscillatory chromatid movements are that they result from an underlying oscillator or that they are caused by a stochastic bistable switch. In the following sections, we explore these two scenarios in detail.

A modified design generates a trial-and-error oscillation

All biochemical oscillations rely on some form of negative feedback as well as on a time delay (43). Thus, the original interaction network (Fig. 1 *A*) needs to be modified to account for these features if it should give rise to an oscillation. Without limiting the generality of the foregoing, we chose to implement these features in the most parsimonious way - i.e., without the introduction of new components. (It has to be stressed that this is one way out of many that a negative feedback and a time delay could be realized in the actual biological system; our conclusions are however generally valid, irrespective of the molecular mechanism.)

We introduce two new interactions into the network (Fig. 4 *A*):

First, we assume that Att and S-Att have a positive effect on Eraser and S-Eraser, respectively. This modification introduces the required negative feedback: Att activates Eraser, which in turn inhibits Att. In addition, we create the required time delay by implementing a positive feedback through Eraser self-activation. We analyze the resulting dynamical system analogously to the previous network. To begin, we plot a phase plane of Eraser and Att (Fig. 4 *B*; compare to Fig. 1 *B*).

Again, we plot two cases, i.e., absence and presence of S-Att. Because the modifications of the network affect Eraser only, the Att balance curve remains sigmoid, indicating the repression of Att by increasing Eraser. The Eraser balance curves by contrast are changed compared to the situation shown in Fig. 1 *B*. In the presence of high S-Att, Eraser is now inactive, irrespective of whether Att is high or low: If Att is high, it cooperates with S-Att to create Tension and Eraser is repressed. If Att is low, Eraser does not get activated. The steady state formed by the intersection of the balance curves is stable and corresponds to the bi-oriented state. In the absence of S-Att, Eraser is low if Att is low because it cannot get activated. However, if Att reaches a certain threshold, Eraser gets abruptly activated. The bistable, S-shaped balance curve is caused by Eraser autoactivation.

The steady state formed by the intersection of the balance curves is unstable, and creates a limit cycle oscillation with four overlapping stages (Fig. 4 *B*, *inset*) The trial stage corresponds to low Eraser activity and the initiation of Att. The detecting stage corresponds to the activation of Eraser after Att has increased but failed to generate Tension. The detaching stage corresponds to the inhibition of tensionless Att; (note that high Eraser sustains itself despite a decrease in Att). Lastly, the, resetting stage corresponds to the collapse of Eraser activity and the resetting of the system.

A comparison of the signal-response curve of Att to S-Att illustrates the consequences of the newly added assumptions (Fig. 4 *C*; compare to Fig. 1 *C*). The stable steady state corresponding to the bi-oriented state is preserved, as is the sharp threshold, which helps distinguish correct from incorrect attachment configurations. The main consequence of the new assumptions is that the steady state corresponding to weak KT-MT binding has now been replaced by a trial-and-error oscillation around an unstable steady state. If the communication between sister kinetochores is prevented as in the pseudo-anaphase experiments (34), both kinetochores show sustained oscillations (Fig. 4 *D*).

The trial-and-error oscillator promotes efficient, robust, and faithful chromosome bi-orientation

With a stochastic simulation, we show that the trial-and-error oscillations on isolated kinetochores promote efficient and robust bi-orientation of coupled sister-chromatids (Fig. 4 *E*, compare to Fig. 2 *A*). The reasons for this more efficient and more robust bi-orientation become apparent when we plot the stochastic time-course simulation onto the pseudo-phase plane of the oscillator model (Fig. 4 *F*, compare to Fig. 2 *B*). In contrast to the switch model, which had two stable steady states and thus two attraction basins, the modified system has only a single attractor, which corresponds to the bi-oriented state. Thus, the system is attracted to the bi-orientation state no matter what the initial conditions are. The presence of a global attractor means that bi-orientation can no longer be lost spontaneously. All this was also true for the switch-model, given that we look at a parameter regime that does not cause bistability (Fig. 2 *D*). However, in stark contrast to this previous case, KT-MT binding in the absence of tension is reduced to a very low level by the trial-and-error oscillator. In this way, the trial-and-error oscillator promotes efficient, robust, and faithful bi-orientation.

A stochastic bistable switch dynamically mimics an oscillator

The trial-and-error oscillator is an elegant mechanism to promote bi-orientation; however, it requires a negative feedback loop, which we have introduced by assuming a positive effect of Att on Eraser. In this section, we show that a stochastic bistable switch does not require this assumption (Fig. 5 *A*), and still can mimic the dynamics of a trial-and-error oscillator. In this final scenario, the positive feedback implemented by Eraser autoactivation can result in two stable steady states in the absence of Tension (Fig. 5 *B*). The low Eraser state promotes efficient bi-orientation and the high Eraser state ensures removal of error. In the presence of high Tension, the state with high Eraser activity disappears and the state with low Eraser activity is stabilized (Fig. 5 *B*). A comparison of the signal-response curve of Att to S-Att illustrates the similarities between the stochastic bistable switch and the oscillator (Fig. 5 *C*, compare to Fig. 4 *C*). In the absence of S-Att, stochastic reactions drive Att between a high-level state and a low-level state, just as in a trial-and-error oscillation. If the communication between sister kinetochores is prevented (as in pseudo-anaphase), the stochastic fluctuations of attachments on both kinetochores are less regular compared with the oscillations (Fig. 5 *D*, compare to Fig. 4 *D*). However, similar to the trial-and-error oscillator, a stochastic bistable switch promotes efficient and robust bi-orientation of coupled sister-chromatids (Fig. 5 *E*, compare to Fig. 4 *E*). The reasons are again demonstrated by plotting the stochastic time-course simulation onto the pseudo-phase plane (Fig. 5 *F*). Att is able to increase independent of S-Att, leading the trajectory upward. At high level of Att, the

increase of S-Att causes bi-orientation. In the stochastic switch, the bi-orientation state is not the global attractor as in the trial-and-error oscillator (compare Fig. 5 *F* and Fig. 4 *F*). However, in practice, the bi-orientation is still efficiently maintained, because it is not lost unless both Att and S-Att drop at the same time.

Discussion

Here, we have analyzed the dynamical features of the tension hypothesis of error correction and chromosome bi-orientation. In its minimal form, the hypothesis states that there is a tension-dependent inhibition of an activity, which destabilizes KT-MT attachments, or more generally, decreases the spindle-pulling force that acts on a kinetochore. In dynamical terms, the system is defined by a positive feedback loop between the sister kinetochores of a duplicated chromosome, where attachment on either side stabilizes attachment on the sister side. Depending on the regulatory strengths, this positive feedback loop can give rise to bi-stability. One of the two stable steady states corresponds to a strong attachment (strong Att and S-Att), while the other corresponds to a loose attachment (weak Att and S-Att). This setup allows a robust distinction between incorrect attachment configurations with low tension, which are readily dissolved, and correctly bi-oriented attachment configurations, which are stable. However, the self-stabilizing nature of the steady states causes difficulties in explaining how bi-orientation is initiated, given that the process necessarily must start from a state where both sister kinetochores are unattached. From such initial conditions, the steady state corresponding to weak attachments (and not the steady state corresponding to bi-orientation) is the default attractor. Thus, while a bistable switch model explains some of the features of error correction and bi-orientation, it is not entirely satisfactory and requires modification.

We have shown that the initiation problem can be traced to a separatrix that results from the mutual activation of Att and S-Att. Without excluding other possibilities, we present four ways of modifying the switch model that are all consistent with the tension hypothesis and can all overcome the initiation problem:

1. The system could cross the separatrix via stochastic reactions;

2. KT-MT attachment could be so efficient that the separatrix disappears;

3. The system could give rise to a trial-and-error oscillator; and

4. Stochastic reactions could drive the system to flip between high and low attachment.

We have tested these four modifications of a switch model and have highlighted how they comply with the requirements for efficient bi-orientation (Table 3). Both the oscillator model and the stochastic bistable switch model solve this challenge through dynamical stability of kinetochore-microtubule (KT-MT) in the absence of tension. When the attachment is stable, it opens a time window for the formation of KT-MT attachment at the sister kinetochore and thus formation of tension. However, if a sister attachment fails to form during this time window, the tensionless attachment becomes unstable and gets dissolved.

Table 3 Comparison of the dynamical scenarios for chromosome bi-orientation explored here

Scenario	Deterministic switch-model	Stochastic switch-model	No-switch model	Oscillator model	Stochastic bistable switch
Clear distinction	Yes	Yes	No	Yes	Yes
Stable maintenance	Yes	No	Yes	Yes	Yes
Efficient initiation	No	Yes	Yes	Yes	Yes

To achieve faithful bi-orientation in an error-prone, stochastic cellular system, the amphitelic configuration should be stabilized and erroneous attachments should be dissolved. Previous models have simulated this process by assigning a higher decay rate to erroneous attachments when compared to amphitelic ones (4, 44). In contrast to these previous models, which do not explore possible mechanisms for the assumed different decay rates, our model provides a mechanistic explanation for the distinct stability based on Tension-dependent Eraser inhibition. From our theoretical considerations, we can derive predictions that are experimentally testable. Our models suggest that, in the absence of sister-kinetochore communication (i.e., artificial disruption of cohesion as in the pseudo-anaphase experiments (Fig. 3), Eraser activity at the kinetochore should fluctuate. In molecular terms, Aurora B is a key component of the Eraser activity (16, 17,18, 19) and high Aurora B activity at the outer kinetochore correlates with unstable KT-MT attachments (15, 24). Hence, the dynamical scenarios presented here could be tested by measuring Aurora B activity in the absence of tension, ideally with direct sensors at the outer kinetochore. The activity of Aurora B might be measured with the help of existing Aurora B Förster resonance energy transfer sensors (45). If a direct measurement is too difficult to achieve with currently available techniques, the centromeric localization of Aurora B can potentially be used as a proxy for its kinase activity, as suggested by previous experiments (46).

In human cells, Aurora B is found at significantly increased concentration at misaligned centromeres compared with properly aligned centromeres. This difference disappears upon pharmacological inhibition of Aurora B kinase activity (45). These observations suggest that Aurora B promotes its own accumulation at the centromere through a positive feedback in a kinase-dependent manner. A positive feedback in the control of Aurora B has also been proposed by others (47). This evidence supports the Eraser self-activation assumed in our models. However, it is worth noting that the positive feedback might also arise through mutual inhibition of Eraser and Att, or through self-promotion of Att. Further experimental investigation of the molecular interactions is required to determine the exact mechanism through which bi-orientation is achieved.

In summary, we have identified several possible dynamical routes to bi-orientation that are consistent with the tension hypothesis. Out of these, a trial-and-error oscillation or a stochastic bistable switch seem the best candidates, both exhibiting the desired features and providing an explanation for experimental observations. Further experimental data is required to settle the question of how the dynamical system is really built, and it will be interesting to see whether an oscillatory mechanism or stochastic switching is indeed involved.

Methods

For an explanation of the model variables Attachment (Att), Sister-Attachment (S-Att), Eraser, Sister-Eraser (S-Eraser) and Tension as well as their interactions, see section Results. Here we focus mainly on the technical aspects of the model.

Mathematical form of the models

To extract generic dynamical properties without having to make explicit assumptions regarding the molecular details, we adopt a generic formula to describe the temporal change of each model component *X* as a function of all other model components (31, 32),

$$\frac{dX_i}{dt} = \tau_i(F_i - X_i),$$

τ_i is the timescale at which this steady state is reached. F_i, the steady-state value of the variable X_i, is a dimensionless variable normalized to its maximal value and is given by

$$F_i = \frac{1}{1 + e^{-\sigma W_i}}.$$

The value of F_i correlates positively with the value of W_i, the sum of regulations on the component X_i. Note that W_i can be negative (inactivation) or positive (activation), but F_i is always positive. F_i is suitable for describing a dimensionless variable, which tends toward 1 if W_i is large and positive and toward 0 if W_i is large and negative (31, 32).

W_i is the net effect of all regulations on the variable X_i and is given by

$$W_i = R_0^i + \sum_j R_j^i \cdot X_j,$$

where R_0^i is the background regulation and R_j^i is the regulation exerted by entity j. The coefficient R_j^i is negative if j inhibits i; positive if j activates i; and 0 if $j$does not regulate i. In this way, switching values of R_j^i between zero and nonzero values allows easy exploration of different network structures. The parameter σcontrols the nonlinearity of the response to the net regulatory effect W_i. Model equations and parameter values are presented in Table 1, Table 2.

Table 1 Model equations

Att	Eraser	Tension
$\frac{dATT}{dt} = \tau_a$	$\frac{dERA}{dt} = \tau_{era} \cdot (F_{era} -$	$\frac{dTEN}{dt} = \tau_{ten} \cdot (F_t$
$F_{att} = \frac{1}{1 + e}$	$F_{era} = \frac{1}{1 + e^{-\sigma \cdot W_{era}}}$	$F_{ten} = \frac{1}{1 + e^{-\sigma \cdot}}$
$W_{att} = R_0^{att}$	$W_{era} = R_0^{era} + R_{ten}^{era} \cdot TI$	$W_{ten} = R_0^{ten} + R_b^t$

Table 2 Parameter values

Shared parameters	Model-specific parameters									
$R_{ten}^{era} = -$	Parameter	R_0^{att}	R_{att}^{era}	R_0^{era}	R_{era}^{era}	R_{bip}^{ten}	σ	τ_{att}	τ_{era}	τ_{ten}
$R_0^{ten} = -$	Switch mod	0.55	0	0.3	0	1	5	1	1	10

$R_{era}^{att} = -$	el									
	Nonswitch model	0.8	0	0.3	0	1	5	1	1	10
	Oscillator model	0.55	0.5	−0.75	1	1	10	1	1	10
	Stochastic bistable switch model	0.55	0	−0.75	2	10	5	10	10	1

To incorporate the effects of stochastic reactions, we used Gillespie's algorithm (33). The model includes the five components Att, S-Att, Eraser, S-Eraser, and Tension, whose production and destruction are described in 10 elementary reactions. We use p_{10} to describe the sum of the rates of all 10 reactions. The time interval τ after which the next reaction occurs is computed as

$$\tau = \frac{1}{p_{10}} \ln\left(\frac{1}{r_1}\right),$$

where r_1 is a uniformly distributed random number from the unit interval [0, 1]. To determine which reaction occurs, we select the reaction of index n with

$$p_n > r_2\, p_{10},$$
$$p_{n-1} \leq r_2\, p_{10},$$

where p_n is the sum of rates of the first n reactions and r_2 is a uniformly distributed random number from the unit interval [0, 1]. Parameters are set such that each stochastic reaction brings 5% change to the variable. Different noise intensities (10 or 2.5%, respectively) gave similar results.

Calculation of phase planes and signal response curves

For phase-plane analysis of the dynamics of Att and Eraser at a single kinetochore (Figs. 1 *B* and 4 *B*), their differential equations were used. Tension was computed at its steady-state (Tension = F_{ten}). S-Att was used as a parameter and is either 0 or 1. S-Eraser does not affect the shapes of these diagrams and is set to 0. For phase-plane analysis on the interaction of Att and S-Att (Figs. 1 *D* and 2 *D*), their differential equations were used; all other variables were computed at their steady states. To calculate the signal response curves (Figs. 1 *C*, 2 *C*, 4 *C*, and 5 *C*), the differential equations of Att, Eraser, and

Tension were used. S-Att was varied as a parameter. S-Eraser does not affect the curves in these diagrams and is set to 0. For pseudo-phase plane analysis on the interaction of Att and S-Att (Figs. 2 *B*, 4 *F*, and 5 *F*), the two signal response curves are plotted on the same plane.

Analysis of experimental data

Chromatid movements in the absence of tension were recorded for 800 s (34), from which the chromatid positions were extracted and plotted. The position of each chromosome is recorded as (x_n, x_y) every 5 s (160 data points). The first position (x_1, y_1) is used as a reference point and the distances of the centromere from this reference point are computed at each time point by

$$D_n = \sqrt{(x_n - x_1)^2 + (y_n - y_1)^2}.$$

Velocities of chromatid movements

To reduce sampling error, 11 consecutive distance values were averaged into an average distance (AD),

$$AD_n = \frac{1}{11} \sum_{i=n-5}^{n+5} D_i,$$
$$n = [6, 7, 8, \ldots, 155].$$

The average velocity V_n in a 5-s interval is then computed as

$$V_n = \frac{A_{n+1} - A_n}{5}.$$

Acknowledgments

We thank John Tyson for critically reading the manuscript, as well as members of the Novák laboratory, in particular Maria Rosa Domingo Sananes, for helpful discussions and advice.

This work was supported by grants from the European Community's Seventh Framework Program (UniCellSys and MitoSys). T.Z. carried out part of the work while visiting the Kavli Institute for Theoretical Physics, and thanks the staff there for their hospitality and support (grant No. NSF PHY11-25915).

References

1. Murray, A. W. 2011. A brief history of error. Nat. Cell Biol. 13:1178– 1182.

2. Nicklas, R. B. 1997. How cells get the right chromosomes. Science. 275:632–637.

3. Nicklas, R. B., and S. C. Ward. 1994. Elements of error correction in mitosis: microtubule capture, release, and tension. J. Cell Biol. 126:1241–1253.

4. Paul, R., R. Wollman, ., A. Mogilner. 2009. Computer simulations predict that chromosome movements and rotations accelerate mitotic spindle assembly without compromising accuracy. Proc. Natl. Acad. Sci. USA. 106:15708–15713.

5. Scholey, J. M., I. Brust-Mascher, and A. Mogilner. 2003. Cell division. Nature. 422:746–752.

6. Nasmyth, K. 2002. Segregating sister genomes: the molecular biology of chromosome separation. Science. 297:559–565.

7. Oliveira, R. A., and K. Nasmyth. 2010. Getting through anaphase: splitting the sisters and beyond. Biochem. Soc. Trans. 38:1639–1644.

8. Indjeian, V. B., and A. W. Murray. 2007. Budding yeast mitotic chromosomes have an intrinsic bias to biorient on the spindle. Curr. Biol. 17:1837–1846.

9. Loncarek, J., O. Kisurina-Evgenieva, ., A. Khodjakov. 2007. The centromere geometry essential for keeping mitosis error free is controlled by spindle forces. Nature. 450:745–749.

10. Magidson, V., C. B. O'Connell, ., A. Khodjakov. 2011. The spatial arrangement of chromosomes during prometaphase facilitates spindle assembly. Cell. 146:555–567.

11. Wollman, R., E. N. Cytrynbaum, ., A. Mogilner. 2005. Efficient chromosome capture requires a bias in the 'search-and-capture' process during mitotic-spindle assembly. Curr. Biol. 15:828–832.

12. Ault, J. G., and C. L. Rieder. 1992. Chromosome mal-orientation and reorientation during mitosis. Cell Motil. Cytoskeleton. 22:155–159.

13. Cimini, D., B. Howell, ., E. D. Salmon. 2001. Merotelic kinetochore orientation is a major mechanism of aneuploidy in mitotic mammalian tissue cells. J. Cell Biol. 153:517–527.

14. Carmena, M., S. Ruchaud, and W. C. Earnshaw. 2009. Making the Auroras glow: regulation of Aurora A and B kinase function by interacting proteins. Curr. Opin. Cell Biol. 21:796–805.

15. Kelly, A. E., and H. Funabiki. 2009. Correcting aberrant kinetochore microtubule attachments: an Aurora B-centric view. Curr. Opin. Cell Biol. 21:51–58.

16. Ditchfield, C., V. L. Johnson, ., S. S. Taylor. 2003. Aurora B couples chromosome alignment with anaphase by targeting BubR1, Mad2, and Cenp-E to kinetochores. J. Cell Biol. 161:267–280.

17. Hauf, S., R. W. Cole, ., J. M. Peters. 2003. The small molecule Hesperadin reveals a role for Aurora B in correcting kinetochore-microtubule attachment and in maintaining the spindle assembly checkpoint. J. Cell Biol. 161:281–294.

18. Kallio, M. J., M. L. McCleland, ., G. J. Gorbsky. 2002. Inhibition of Aurora B kinase blocks chromosome segregation, overrides the spindle checkpoint, and perturbs microtubule dynamics in mitosis. Curr. Biol. 12:900–905.

19. Lampson, M. A., K. Renduchitala, ., T. M. Kapoor. 2004. Correcting improper chromosome-spindle attachments during cell division. Nat. Cell Biol. 6:232–237.

20. Cimini, D. 2007. Detection and correction of merotelic kinetochore orientation by Aurora B and its partners. Cell Cycle. 6:1558–1564.

21. Li, X., and R. B. Nicklas. 1995. Mitotic forces control a cell-cycle checkpoint. Nature. 373:630–632.

22. Dewar, H., K. Tanaka, ., T. U. Tanaka. 2004. Tension between two kinetochores suffices for their biorientation on the mitotic spindle. Nature. 428:93–97.

23. Tanaka, T., J. Fuchs, ., K. Nasmyth. 2000. Cohesin ensures bipolar attachment of microtubules to sister centromeres and resists their precocious separation. Nat. Cell Biol. 2:492–499.

24. Lampson, M. A., and I. M. Cheeseman. 2011. Sensing centromere tension: Aurora B and the regulation of kinetochore function. Trends Cell Biol. 21:133–140.

25. Liu, D., G. Vader, ., S. M. Lens. 2009. Sensing chromosome bi-orientation by spatial separation of aurora B kinase from kinetochore substrates. Science. 323:1350–1353.

26. Sandall, S., F. Severin, ., A. Desai. 2006. A Bir1-Sli15 complex connects centromeres to microtubules and is required to sense kinetochore tension. Cell. 127:1179–1191.

27. Nicklas, R. B., and C. A. Koch. 1969. Chromosome micromanipulation. 3. Spindle fiber tension and reorientation of mal-oriented chromosomes. J. Cell Biol. 43:40–50.

28. Cimini, D., B. Moree, ., E. D. Salmon. 2003. Merotelic kinetochore orientation occurs frequently during early mitosis in mammalian tissue cells and error correction is achieved by two different mechanisms. J. Cell Sci. 116:4213–4225.

29. Gay, G., T. Courtheoux, ., Y. Gachet. 2012. A stochastic model of kinetochore-microtubule attachment accurately describes fission yeast chromosome segregation. J. Cell Biol. 196:757–774.

30. Gregan, J., S. Polakova, ., D. Cimini. 2011. Merotelic kinetochore attachment: causes and effects. Trends Cell Biol. 21:374–381.

31. Tyson, J. J., and B. Novak. 2010. Functional motifs in biochemical reaction networks. Annu. Rev. Phys. Chem. 61:219–240.

32. Mjolsness, E., D. H. Sharp, and J. Reinitz. 1991. A connectionist model of development. J. Theor. Biol. 152:429–453.

33. Gillespie, D. T. 1976. A general method for numerically simulating the stochastic time evolution of coupled chemical reactions. J. Comput. Phys. 22:403–434.

34. Oliveira, R. A., R. S. Hamilton, ., K. Nasmyth. 2010. Cohesin cleavage and Cdk inhibition trigger formation of daughter nuclei. Nat. Cell Biol. 12:185–192.

35. Vazquez-Novelle, M. D., and M. Petronczki. 2010. Relocation of the chromosomal passenger complex prevents mitotic checkpoint engagement at anaphase. Curr. Biol. 20:1402–1407.

36. Cheeseman, I. M., J. S. Chappie, ., A. Desai. 2006. The conserved KMN network constitutes the core microtubule-binding site of the kinetochore. Cell. 127:983–997.

37. DeLuca, J. G., W. E. Gall, ., E. D. Salmon. 2006. Kinetochore microtubule dynamics and attachment stability are regulated by Hec1. Cell. 127:969–982.

38. Andrews, P. D., Y. Ovechkina, ., J. R. Swedlow. 2004. Aurora B regulates MCAK at the mitotic centromere. Dev. Cell. 6:253–268.

39. Lan, W., X. Zhang, ., P. T. Stukenberg. 2004. Aurora B phosphorylates centromeric MCAK and regulates its localization and microtubule depolymerization activity. Curr. Biol. 14:273–286.

40. Mirchenko, L., and F. Uhlmann. 2010. Sli15(INCENP) dephosphorylation prevents mitotic checkpoint reengagement due to loss of tension at anaphase onset. Curr. Biol. 20:1396–1401.

41. Wollman, R., G. Civelekoglu-Scholey, ., A. Mogilner. 2008. Reverse engineering of force integration during mitosis in the Drosophila embryo. Mol. Syst. Biol. 4:195. Biophysical Journal 104(12) 2595–2606 Dynamical Scenarios for Chromosome Bi-orientation 2605

42. Parry, D. H., G. R. Hickson, and P. H. O'Farrell. 2003. Cyclin B destruction triggers changes in kinetochore behavior essential for successful anaphase. Curr. Biol. 13:647–653.

43. Novak, B., and J. J. Tyson. 2008. Design principles of biochemical oscillators. Nat. Rev. Mol. Cell Biol. 9:981–991.

44. Mistry, H. B., D. E. MacCallum, ., F. A. Davidson. 2008. Modeling the temporal evolution of the spindle assembly checkpoint and role of Aurora B kinase. Proc. Natl. Acad. Sci. USA. 105:20215–20220.

45. Salimian, K. J., E. R. Ballister, ., B. E. Black. 2011. Feedback control in sensing chromosome biorientation by the Aurora B kinase. Curr. Biol. 21:1158–1165.

46. Fuller, B. G., M. A. Lampson, ., T. M. Kapoor. 2008. Midzone activation of Aurora B in anaphase produces an intracellular phosphorylation gradient. Nature. 453:1132–1136.

47. Wang, F., N. P. Ulyanova, ., J. M. Higgins. 2011. A positive feedback loop involving Haspin and Aurora B promotes CPC accumulation at centromeres in mitosis. Curr. Biol. 21:1061–1069.

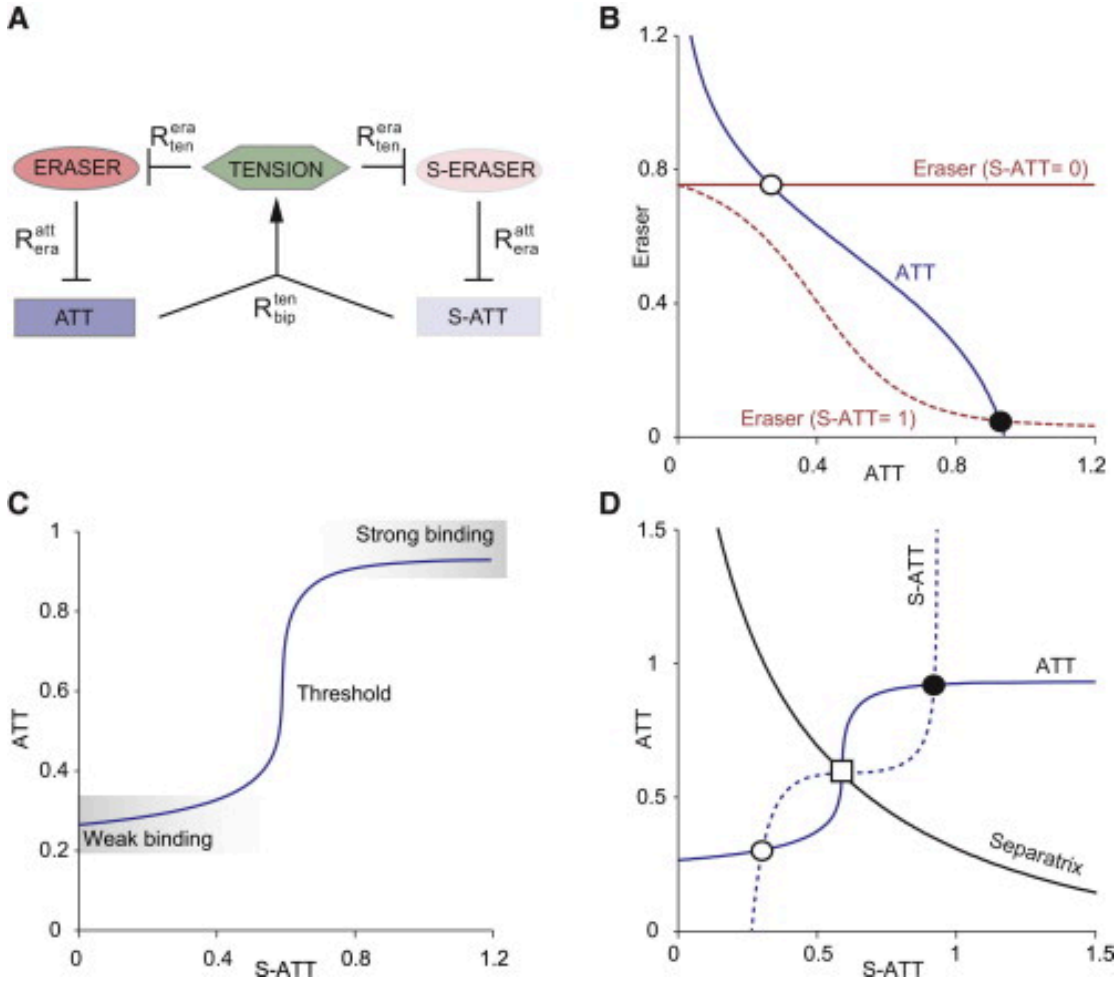

Figure 1

A minimal network representation of the tension hypothesis and its dynamical properties. (*A*) Network diagram. On both kinetochores, Eraser represses Att. After the formation of bi-orientation, Att and S-Att together generate Tension to repress Eraser and S-Eraser. (*B*) The mutual antagonism between Att and Eraser. The interaction between Att and Eraser is investigated on a phase plane. The balance curves for Att (*blue line*) and Eraser (*red lines*) are plotted in the absence and the presence of S-Att. Att decreases when Eraser activity increases. In the absence of S-Att, Eraser has constant activity (*red line*) and the steady state is characterized by high Eraser activity and low Att (loose attachment, *open circle*). In the presence of high S-Att, Eraser is repressed by increasing Att (*red dashed line*) and the steady state corresponds to strong binding (*solid circle*). (*C*) The response of Att to different levels of S-Att. Att and S-Att are either both low or both high. These two states are separated by a threshold. (*D*) Phase-plane analysis of the mutual activation between Att and S-Att. The balance curve of Att (*solid blue line*) and of S-Att (*dashed blue line*) are plotted. Two steady states are surrounded by two attraction basins that are separated by a separatrix (*black line*), which originates from a saddle point (*open square*). (*Lower-left steady state*) Loose attachment (*open circle*); (*upper right*) strong attachment (*solid circle*).

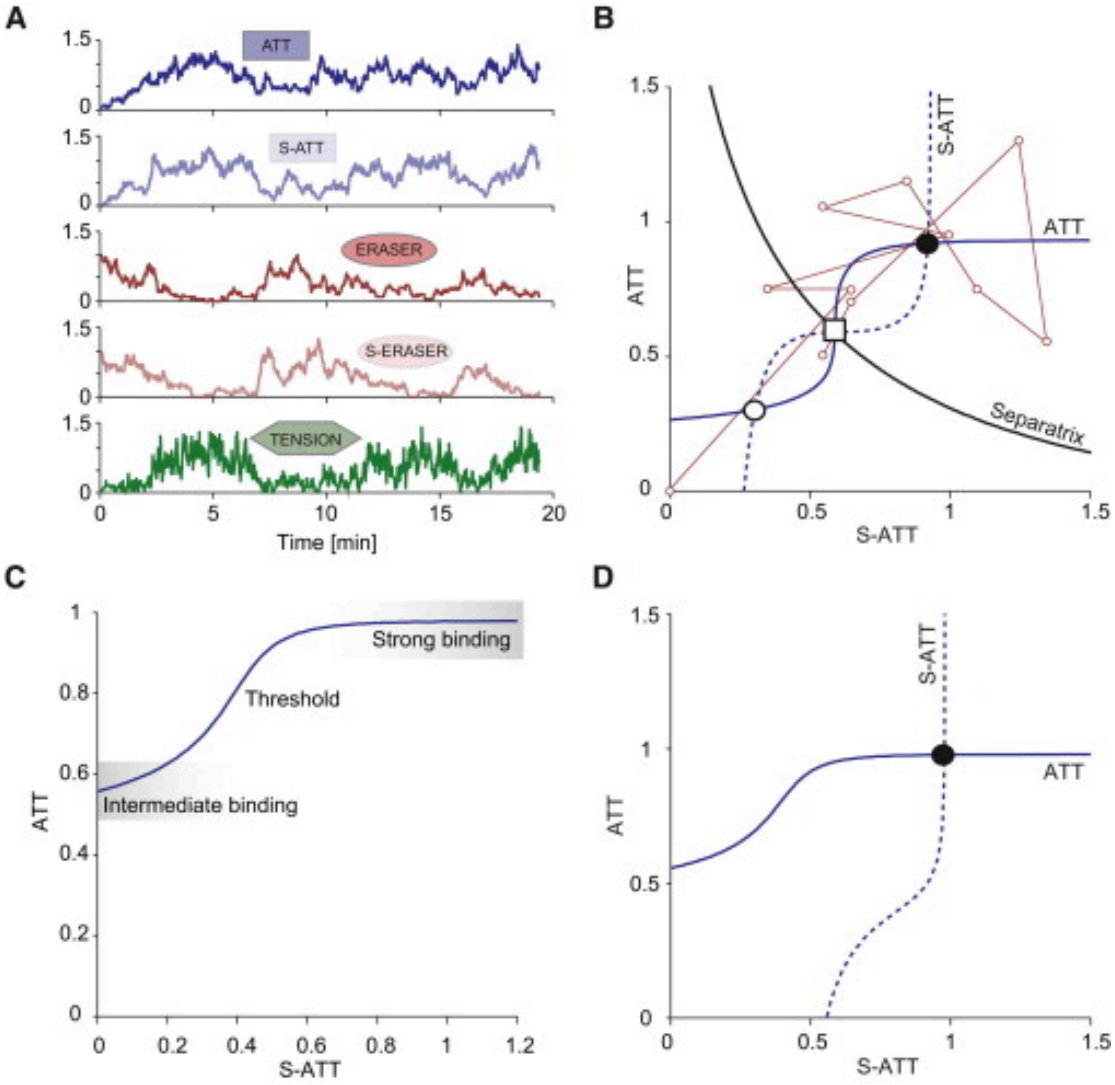

Figure 2

Two ways of overcoming the initiation problem of the bistable switch model. (*A*) Stochastic effects can initiate bi-orientation. Representative stochastic time-series simulation. All five variables of the model are shown. (*B*) Phase-plane plotting of the stochastic trajectory. (*Red line* and *circles*) Replotting of the time-dependent changes of Att and S-Att sampled from the representative simulation shown in panel *A* on the phase plane shown in Fig. 1 *D*. Note that the trajectory crosses back and forth over the separatrix, indicating that the system can move between the two attraction basins. (*C* and *D*) Bi-orientation can be the only steady state if significant attachment can form already in the absence of tension. (*C*) Signal-response curve. Note the reduced dynamic range when compared to Fig. 1 *C*. (*D*) Phase plane. The diagram corresponds to Fig. 1 *D*, but with $R_0^{att} = 0.8$ instead of $R_0^{att} = 0.55$. One steady state has disappeared and the system is mono-stable. The bi-oriented configuration has become a global attractor.

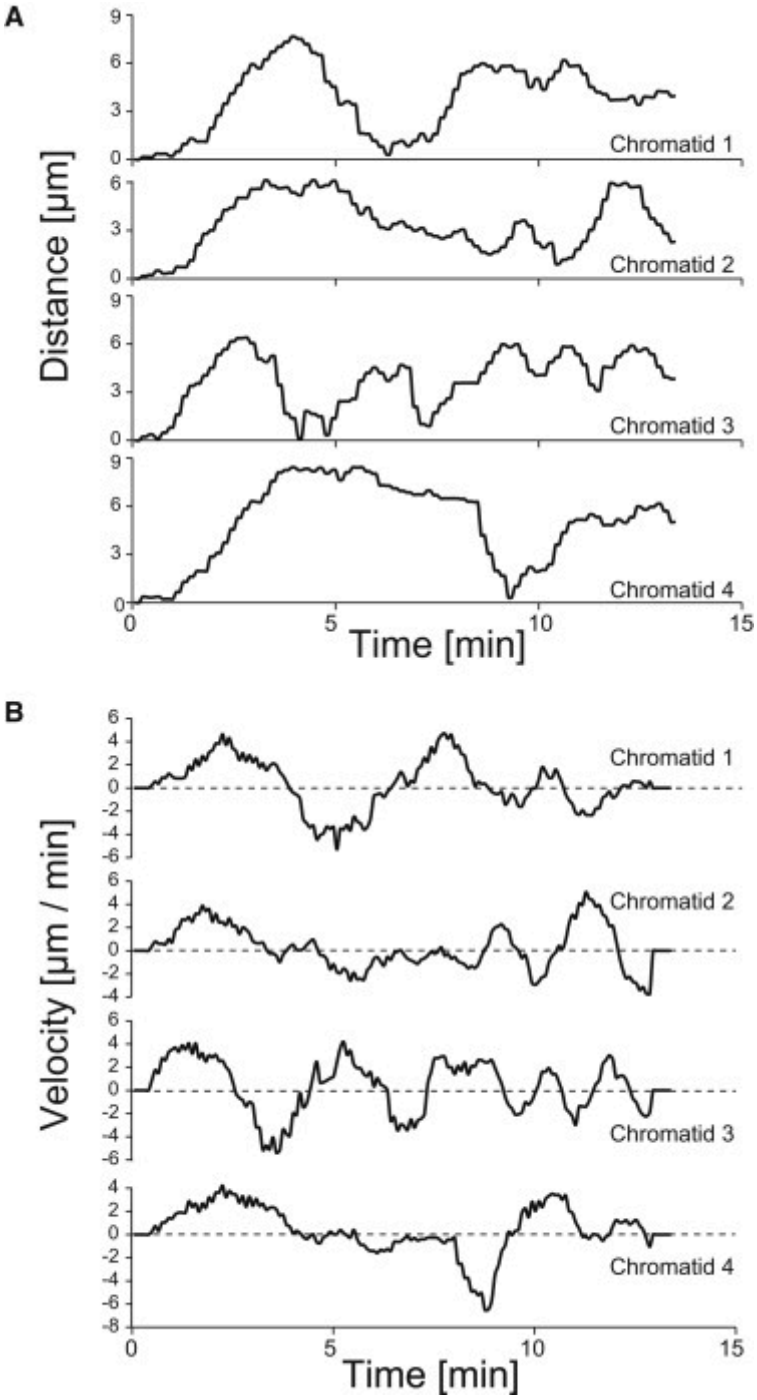

Figure 3

Isolated chromatids show oscillatory movements. Reanalysis of experimental data (34) in pseudo-anaphase (see main text for details). (*A*) Distances from an initial reference point are plotted for four distinct isolated chromatids. (*B*) The velocities of the chromatids shown in panel *A*.

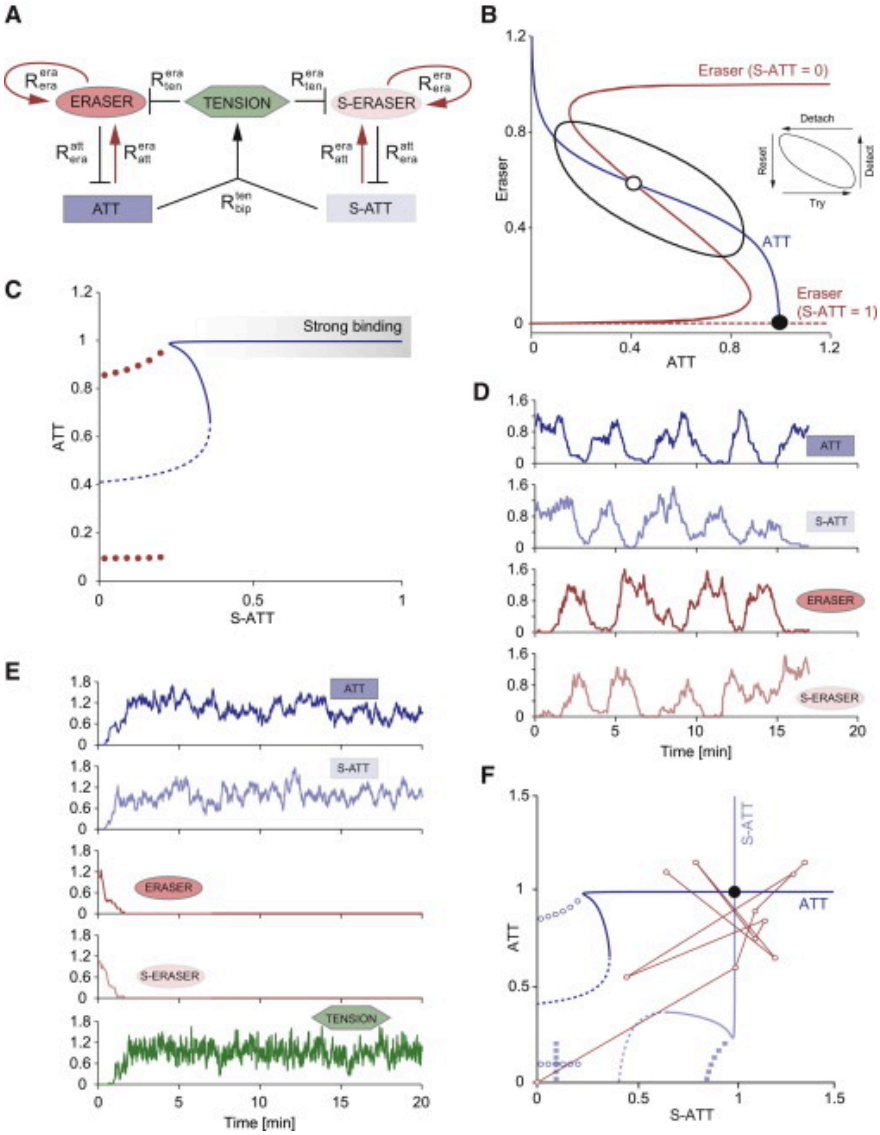

Figure 4

A trial-and-error oscillator. (*A*) Modified network diagram. Compared with the initial network in Fig. 1 *A*, Eraser activity is now promoted by Att, and Eraser promotes its own activity (*red arrows*). These modifications create a negative feedback loop and a time delay, which are required features of an oscillator. (*B*) Phase-plane analysis of the oscillator model. Phase plane as inFig. 1 *B*, but for the oscillator model. In the absence of S-Att, the intersection between the Att balance curve (*blue line*) and the Eraser balance curve (*red line*) results in an unstable steady state (*open circle*) and a limit cycle oscillation (*black line*). (*Inset*) The different phases of the oscillation. If S-Att is high, the intersection between the Att balance curve and the Eraser balance curve (*red dashed line*) results in a stable steady state with high Att (*solid circle*). (*C*) Signal response curve. If S-Att is below a critical threshold, the steady states are unstable (*dashed part* of the *blue curve*) and Att oscillates between the indicated minima and maxima (*red dots*). At suprathreshold levels of S-Att, the oscillation stops and a branch with stable steady states characterized by high Att appears (*solid part* of the *blue curve*). (*D* and *E*) Time-course plotting of representative stochastic simulations. (*D*) If the communication between sister kinetochores is disrupted (no tension is created), Att and Eraser, as well as S-Att and S-Eraser, show oscillations. (*E*) If sisters communicate with each other, Tension is quickly generated and it is maintained throughout (compare to Fig. 2 *A*). A bi-oriented state is thus efficiently initiated and robustly maintained. (*F*) Pseudo-phase plane plotting. The signal response curve (*C*) is plotted as the Att balance curve, while the S-Att balance curve is a mirror picture. The maximal and minimal values of the Att oscillation (*circles*) and S-Att (*squares*) are indicated. (*Black solid circle*) The only stable steady state corresponding to bi-orientation. (*Red circles* and *lines*) Replotting of the time-dependent changes of Att and S-Att sampled from the representative simulation shown in panel *E*.

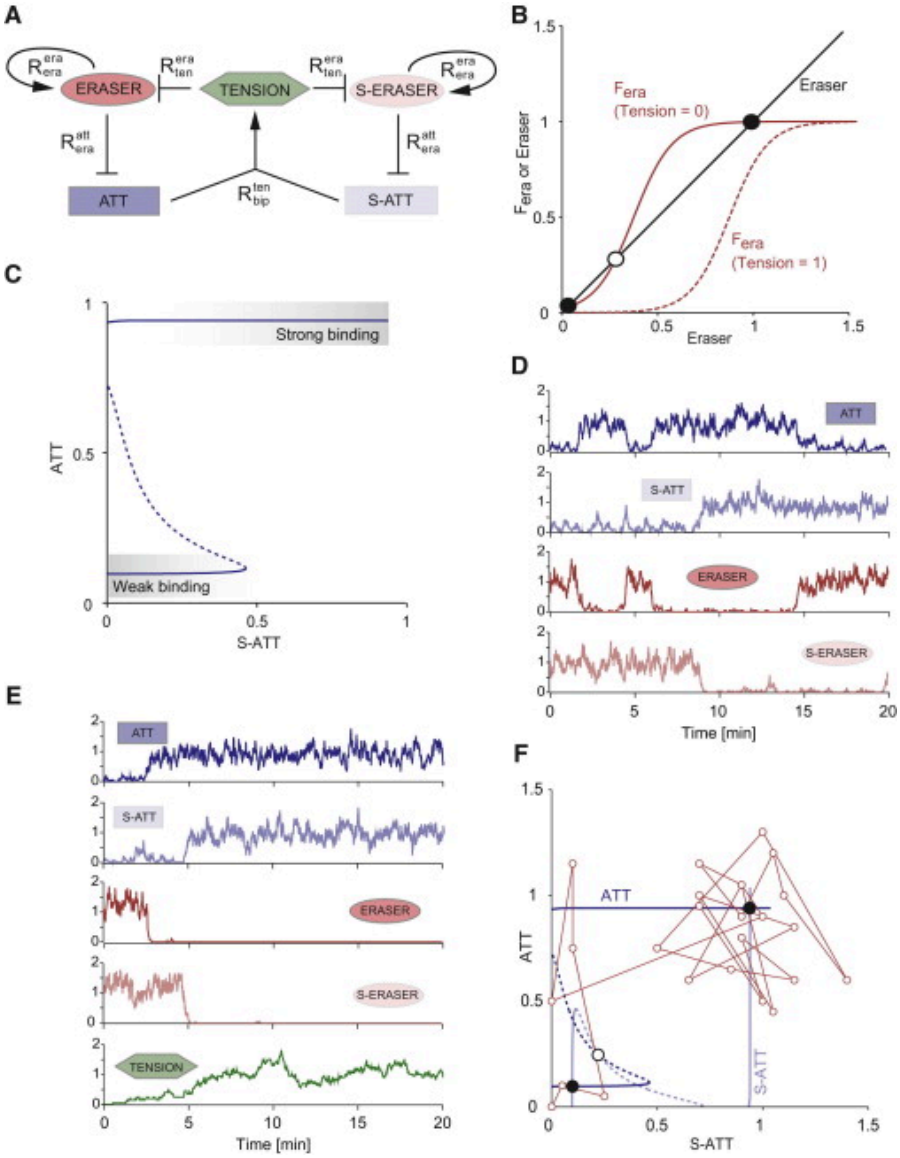

Figure 5

A stochastic bistable switch. (*A*) Network diagram. The positive feedback is implemented with Eraser self-activation. Compared to the oscillator model, the assumption of a negative feedback between Eraser and Att is dropped. (*B*) Analysis of the model. In the absence of Tension, the intersection between the eraser steady state (F_{era}, *solid red*) and Eraser (*black*) results in two stable steady states (*solid circles*) separated by an unstable steady state (*open circle*). If Tension is high, the intersection between Eraser steady state (F_{era}, *dashed red*) and Eraser results in one stable steady state with inactive Eraser (*solid circle*). (*C*) Signal response curve. If S-Att is below a critical threshold, stable steady states (*solid parts* of the *curve*) with either low or high Att are separated by unstable steady states (*dashed part* of the*curve*). At suprathreshold levels of S-Att, the stable steady state with low Att disappears. (*D* and *E*) Time-course plotting of representative stochastic simulations. (*D*) In the absence of tension, i.e., if the communication between sister kinetochores is disrupted, Eraser activity switches on and off in a stochastic manner. (*E*) If sisters communicate with each other, tension is generated and maintained. A desired bi-oriented state is thus initiated and maintained. Note that low Eraser activity allows a time window during which Att can increase independently of S-Att. (*F*) Pseudo-phase plane plotting. The signal response curve (*C*) is plotted as the Att balance curve, while the S-Att balance curve is a mirror picture. (*Black solid circle*) Stable steady states. (*Top-right steady state*) bi-orientation. (*Red circles* and *line*) Time-dependent changes of Att and S-Att sampled from the representative simulation shown in panel *E*.